

Homoharringtonine inhibits the progression of hepatocellular carcinoma by suppressing the PI3K/AKT/GSK3 β /Slug signaling pathway

Hong-Yuan LIU, Tian-Xiu DONG, Zi-Zhuo LI, Tian-Tian LI, Jian JIANG, Ming-Wei ZHU, Ting-Ting AN, Yao-Dong CHEN, Xiu-Hua YANG*

Department of Abdominal Ultrasonography, The First Affiliated Hospital of Harbin Medical University, Harbin, China

*Correspondence: yangxiuhua@hrbmu.edu.cn

Received January 13, 2021 / Accepted March 29, 2021

Homoharringtonine (HHT), was first isolated from the bark of *Cephalotaxus harringtonia* (Knight ex J. Forbes) K. Koch and *Cephalotaxus fortunei* Hook trees. The bark extract is used to treat leukemia and in recent years has also been used in traditional Chinese medicine (TCM) to treat solid tumors. However, the inhibitory mechanism of HHT in the progression of hepatocellular carcinoma (HCC) is rarely studied. We aimed to evaluate the antitumor efficacy of HHT on HCC *in vitro* and *in vivo* and elucidate the underlying molecular mechanism(s). HCC cell lines, including HCCLM3, HepG2, and Huh7, were used to evaluate the antitumor efficacy of HHT *in vitro*. Cytotoxicity and proliferative ability were evaluated by MTT and colony formation assays. Cell cycle progression and apoptosis in HHT-treated HCC cells were evaluated by flow cytometry. To determine the migration and invasion abilities of HCC cells, wound-healing and Transwell assays were used. Finally, western blot analysis was used to reveal the proteins involved. We also established a xenograft nude mouse model for *in vivo* assessments of the preclinical efficacy of HHT, mainly using hematoxylin and eosin staining, immunohistochemistry, ultrasound imaging (USI), and magnetic resonance imaging (MRI). HHT suppressed the proliferation, migration, invasion, and epithelial-mesenchymal transition (EMT) of HCC cells, and induced cell cycle arrest at the G2 phase and apoptosis. In the HCC xenograft model, HHT showed an obvious tumor-suppressive effect. Surprisingly, Slug expression was also decreased by HHT via the PI3K/AKT/GSK3 β signaling pathway at least partially suppressed the growth of HCC via the PI3K/AKT/GSK3 β /Slug signaling pathway.

Key words: homoharringtonine, hepatocellular carcinoma, EMT, PI3K/AKT/GSK3 β /Slug signaling pathway

Hepatocellular carcinoma (HCC) is a common malignant tumor with the sixth and third highest incidence and mortality, respectively, among all tumors [1]. Patients with an early-stage HCC can be treated by surgical resection, liver transplantation, and other methods but patients with advanced unresectable or metastatic HCC have a poor prognosis, which is mainly due to intrahepatic and extrahepatic metastasis and postoperative recurrence of residual tumors [2]. Only a few chemotherapy drugs have been proven effective. Sorafenib, a multikinase inhibitor, is the only systemic therapy that can improve the survival of patients with advanced HCC [3]. Although molecular targeted drugs represented by sorafenib have made major breakthroughs in the treatment of HCC, in recent years, clinical observations have found that approximately 70% of patients are either resistant to sorafenib or develop a series of serious adverse reactions [4]. Therefore, the development of new, highly effective drugs targeting HCC with low toxicity has become an urgent need in the medical community.

In a variety of cancers, the stage of the malignancy and the related mortality are associated with the metastatic ability of the local primary tumor [5]. Epithelial-mesenchymal transition (EMT) is a multi-step biological process that converts polarized epithelial cells into mesenchymal cells, which is closely related to the activities of tumor migration and invasion [6]. EMT has become the primary mechanism for promoting malignant progression and metastatic colonization of epithelial-derived cancers (such as HCC) [7–9]. Notably, a group of transcription factors known as EMT regulators (such as Snail, Slug, Twist, ZEB1, and ZEB2) can precisely manipulate the EMT process and control the proliferation, migration, invasion, apoptosis, cell stemness, and radio/chemical sensitivity of EMT-related cancer cells [10–12].

Various developmental signaling pathways, such as the phosphoinositide 3-kinase (PI3K)/AKT, nuclear factor- κ B (NF- κ B), Notch, and Wnt/ β -catenin pathways, induce EMT [7, 8]. The PI3K/AKT signaling pathway is one of the

most important pathways in tumors [13], as it plays a vital role in carcinogenesis and tumor progression by inhibiting apoptosis and promoting cell proliferation [14, 15]. PI3K phosphorylates phosphatidylinositol (4,5)-bisphosphate to form phosphatidylinositol (3,4,5)-triphosphate, which functions to prevent apoptosis. AKT is a core serine/threonine kinase downstream of PI3K and has been proven to be a key mediator of HCC cell resistance [16]. Activated AKT phosphorylates glycogen synthase kinase 3 β (GSK3 β), which is an isoform of a serine/threonine kinase and can regulate multiple functions of cells, including apoptosis [17].

In recent years, many natural products and their derivatives, such as vinca alkaloids, taxanes, and camptothecins, have been used in cancer chemotherapy. Moreover, the scientific community in Western countries has also identified the underlying plants linked to these natural products, especially the latent natural products of medicinal plants used in traditional Chinese medicine (TCM) [18]. Homoharringtonine (HHT) was firstly extracted from *Cephalotaxus harringtonia* (Knight ex J. Forbes) K. Koch and *Cephalotaxus fortunei* Hook [19] and has been used clinically to treat leukemia [20]. In recent years, HHT has also been used in research on various solid tumors, such as bladder, kidney, lung, and colorectal cancer [21–24]. Recent studies have reported that HHT suppresses tumor proliferation and migration by regulating EphB4-mediated β -catenin loss in HCC [25]. In this study, we also observed the inhibitory effect of HHT on the growth and metastasis of HCC *in vivo* and *in vitro*. In addition, we found that the inhibitory effect of HHT on HCC is mediated through the PI3K/AKT signaling pathway.

Materials and methods

Compound and reagents. HHT (catalogue number H111922) was purchased from Aladdin Industries (Shanghai, China). The powdered HHT was dissolved in DMSO into a stock solution of 20 mmol/l before use. The primary antibodies used to detect PI3K (CST#4292), p-PI3K (CST#4228), AKT (CST#9272), p-AKT (CST#9271), GSK3 β (CST#9315) and p-GSK3 β (CST#9336) were provided by Cell Signaling Technology (Denver, Massachusetts, USA). The primary antibodies used to detect E-cadherin (Cat No.20874-1-AP), N-cadherin (Cat No.22018-1-AP), Vimentin (Cat No.10366-1-AP), CyclinB1 (Cat No.55004-1-AP), Bax (Cat No.50599-2-Ig), Bcl-2 (Cat No.12789-1-AP), Snail (Cat No.13099-1-AP), Slug (Cat No.12129-1-AP), Twist (Cat No.11752-1-AP), and β -actin (Cat No.66009-1-Ig) were purchased from Proteintech Group (Wuhan, China). The HRP-conjugated AffiniPure goat anti-rabbit IgG (SA00001-2) and AffiniPure goat anti-mouse IgG (SA00001-1) secondary antibodies were obtained from Proteintech Group.

Cell culture. Human liver cells (L-02) and HCC cell lines (HCCLM3, HepG2, and Huh7) were all sourced from the Shanghai Cell Resource Centre (Shanghai, China) and cultured in DMEM containing 10% fetal bovine serum

(FBS) and 1% streptomycin/penicillin solution. All cells were cultured in a 37°C incubator containing 5% CO₂.

MTT assay. The cytotoxicity of HHT was evaluated by the MTT assay. HCCLM3, HepG2, and Huh7 cells were incubated in a 96-well plate at a density of 3000–5000 cells/well and treated with different doses of HHT (0–100 nM) for 24–72 h. Next, MTT solution (5 mg/ml, 20 μ l/well) (Sigma-Aldrich, Merck KgaA, Darmstadt, Germany) was incubated for 4 h, after which 100 μ l of DMSO was added into each well to dissolve the formazan crystals. The absorbance of each well at 490 nm was measured on a microplate reader (Elx808, BioTek Instruments, Winooski, VT, USA). The following formula was used to calculate the inhibition rate of cell proliferation: inhibition rate (%) = $[1 - A_{490}(\text{test})/A_{490}(\text{blank})] \times 100\%$. The experiment was performed in triplicate.

Colony formation assay. After HCC cells were seeded (500 cells/dish) in a 6-cm Petri dishes and cultured for 24 h, treated with different doses of HHT (0–20 nM) for 3 h and then cultured with fresh complete medium, which was replaced every 2 days. After 2 weeks, the cells were fixed with methanol and stained with 0.5% crystal violet. The colonies were all counted manually in three fields (10 \times , Olympus Co., Tokyo, Japan). The experiment was performed in triplicate.

Cell cycle assay. HCC cells seeded in a 6-well plate were treated with HHT (0 or 20 nM) for 48 h, after which they were harvested, fixed with ethanol, stained with propidium iodide (PI), and digested with RNase (10 mg/ml). Finally, flow cytometry was used to determine the cell cycle distribution. The experiment was performed in triplicate.

Apoptosis assay. HCC cells were seeded in a 6-well plate and cultured overnight. After adhering to the surface of the wells, the cells were treated with increasing doses of HHT (0–40 nM) for 48 h. They were then collected, washed, treated with Annexin V-FITC/PI, and incubated in the dark. Finally, flow cytometry was used to detect the apoptosis rate of the HCC cells. The experiment was performed in triplicate.

Wound-healing assay. HCC cells were seeded in 6-well plates to form a monolayer. After the cells were pre-treated with mitomycin C (10 μ g/ml) for 2 h, a scratch was created with a pipette tip, and then the cells were cultured in a serum-free medium and treated with different doses of HHT (0–10 nM). Microscope images were acquired at 0 h, 24 h, and 48 h after scratching. ImageJ software was used to analyze the data. The experiment was performed in triplicate.

Transwell assay. A Transwell chamber (pore size 8 μ m, Corning, Tewkesbury, USA) was used to evaluate the migration and invasion abilities of HCC cells. For the migration assay, HCC cells were pre-treated with different doses of HHT (0–20 nM) for 48 h. Then, the lower compartment of the Transwell chamber was filled with medium containing 10% FBS, and the upper cell was filled with a suspension of pre-treated HCC cells (2 \times 10⁴ cells/well) in serum-free medium (300 μ l). For the invasion assay, the procedure was identical to the migration assay except for the addition of diluted Matrigel (BD Biosciences, Franklin Lakes, NJ, USA)

the upper Transwell chamber to form a continuous layer before the cells were seeded. After 48 h of incubation, the migrated and invading cells were stained with 0.5% crystal violet, observed and analyzed under an optical microscope; images were obtained. The experiment was repeated three times.

Animal tumor model and treatments. BALB/c nude mice (4–5 weeks old) were provided by Charles River, Japan (Beijing, China) and housed in a pathogen-free environment. After they were anaesthetized via intraperitoneal injection of sodium pentobarbital (1%; 5 ml/kg), BALB/c nude mice were subcutaneously inoculated with HCCLM3 cells on the left abdomen to establish a subcutaneous xenograft model. When the tumor size was approximately 200 mm³, tumor-bearing nude mice were randomly divided into two groups (n=4, each group): the control group and the HHT treatment group. The lung metastasis model was established by injecting nude mice with 4×10⁶ cells via tail vein (n=4, each group). The mice in the HHT treatment group received intraperitoneal injections of HHT (10 mg/kg/injection) once every two days. The mice in the control group were intraperitoneally injected with the same volume of phosphate-buffered saline (PBS). During treatment, ultrasound imaging (USI) and magnetic resonance imaging (MRI) was used to monitor tumor changes.

Hematoxylin and eosin staining. After the mice were sacrificed on the 14th day after treatment, the tumors were excised. The main organs (heart, lung, liver, spleen, kidney) were also removed, and then the tumor tissues and organs were fixed with formalin, embedded in paraffin, and sectioned. Subsequently, the sections were deparaffinized and stained with hematoxylin-eosin (H&E) before they were viewed under a microscope and imaged.

Immunohistochemistry. The tissue samples were fixed with formaldehyde and embedded in paraffin before they were sectioned and deparaffinized in water. Antigen retrieval was performed, and specific antibodies were used for immunohistochemical staining with a streptavidin-peroxidase complex. Microscope images were collected.

Ultrasonic imaging. Ultrasound imaging (USI) with an iU Elite ultrasound system (Philips Healthcare, Amsterdam, Netherlands) was conducted to monitor tumor growth and progression. B-mode ultrasound was used to observe tumor size and internal echo, and color Doppler flow imaging (CDFI) and color power Doppler (CPA) were used to evaluate tumor angiogenesis. At the same time, ultrasound elastography (USE) was used to assess the stiffness of the tumor.

MRI. The Philips Achieva 3.0 T TX MR system for MRI examination was used to assess tumor size in nude mice. The imaging sequences include T1WI and T2WI.

Western blot assay. HCC cells seeded in six-well plates were incubated with different doses of HHT (0–40 nM) for 48 h, washed with ice-cold PBS, collected by centrifugation, and lysed with RIPA buffer. Then, the total protein content of HCC cells was obtained by centrifugation and boiling.

The protein concentration was determined by the bicinchoninic acid (BCA) method. Subsequently, the proteins were separated by electrophoresis through a sodium dodecyl sulfate-polyacrylamide gel at constant voltage and then transferred to a PVDF membrane. Then, the membrane was blocked with 5% skim milk/TBST followed by incubation with the corresponding primary and secondary antibodies. Finally, electrochemiluminescence (ECL) reagents (Pierce, Rockford, IL) were used for evaluating the protein band intensities, and ImageJ was used for optical density analysis. The experiment was repeated three times.

Statistical analysis. IBM SPSS 22.0 software was used for statistical analysis. The data are shown as the mean ± standard deviation (X ± SD). Student's t-test or one-way analysis of variance was used to compare differences between two groups or among more than two groups, respectively. A p-value <0.05 was considered statistically significant.

Results

HHT displayed obvious cytotoxicity against HCC cells. First, we observed the cytotoxic effect of HHT on the normal liver cell line L-02 with the MTT assay and found that HHT showed no obvious cytotoxicity in these cells. To identify the potential antitumor activity of HHT on HCC cells, we measured the activity of HCCLM3, HepG2, and Huh7 cells after 24, 48, and 72 h of treatment with different concentrations of HHT (up to 100 nM) using a standard MTT assay. The results indicated that HHT can obviously inhibit the activities of all three HCC cell lines. More importantly, the inhibitory effect of HHT on HCC cells depends on the concentration and duration of HHT treatment. Then, we calculated the 50% inhibitory concentration value (IC₅₀) for 48 h by probit regression analysis. The IC₅₀ values of HHT in HCCLM3, HepG2, and Huh7 cells were approximately 36.85 nM, 18.34 nM, and 19.68 nM. Sorafenib, the most common drug for clinical treatment of HCC, was used as a positive control [26]. The results suggested that HHT and sorafenib could significantly inhibit the growth of HepG2 cells in a dose- and time-dependent manner (Figure 1A). Of note, we calculated the IC₅₀ value of sorafenib at 48 h by probit regression analysis; the value of sorafenib was approximately 5.62 μM, while that of HHT was only 18.34 nM.

HHT inhibits the proliferation of HCC cells. Generally, inhibiting cell proliferation and inducing apoptosis are the main measures by which researchers assess the inhibitory effect of chemotherapy drugs on cancer cell growth [2, 27]. Colony formation can be used to directly reflect the proliferation potential of cells. The evidence of the decline in the proliferative ability of HCC cells treated with HHT was dose-dependent (Figure 1B). Cell proliferation is also related to the normal cell cycle function. Therefore, flow cytometry was used to analyze the cell cycle distribution, study the regulatory effect of HHT on the HCC cell cycle, and further evaluate the mechanism by which HHT

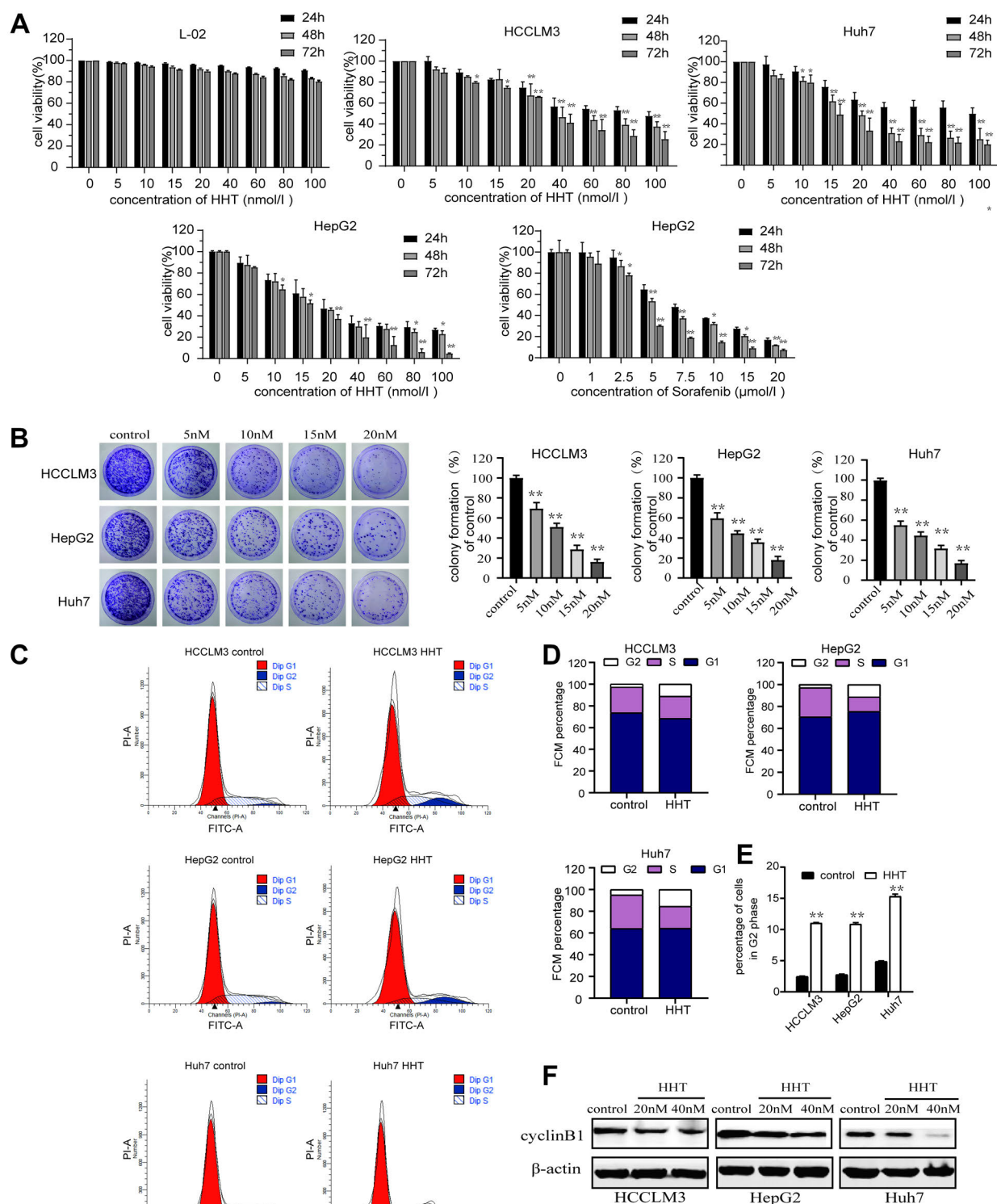


Figure 1. Effect of HHT on the growth of HCC cells. A) Cytotoxic effect of different concentrations of HHT (0–100 nM, 0–72 h) on L-02, HCCLM3, HepG2, and Huh7 cell lines and percentage of surviving HepG2 cells treated with sorafenib (0–20 μM, 0–72 h) as observed by the MTT assay. * $p < 0.05$, ** $p < 0.01$ vs. the control group. B) Colony formation assay was used to verify the growth inhibitory effect of HHT (0–20 nM, 3 h). C–E) Cell cycle analysis of HHT-treated cells showing arrest in G2 phase (20 nM, 48 h). Data are represented as the mean \pm SD ($n = 3$), ** $p < 0.01$. F) Western blot showed that after HHT (0–40 nM, 48 h) treatment, the expression of CyclinB1 was decreased. β -actin was used as the loading control.

inhibits HCC cell proliferation. HHT treatment (20 nM) arrested HCCLM3, HepG2, and Huh7 cells at the G2 phase (Figures 1C, 1D). The proportion of HCCLM3, HepG2, and Huh7 cells in the G2 phase of the HHT treatment group was 4.5, 4, and 3 times higher than that of the corresponding control group, respectively (Figure 1E). We also analyzed the expression levels of cell cycle regulatory proteins by western blot. The expression level of CyclinB1 decreased in a dose-dependent manner after HHT treatment, which was consistent with the cell cycle analysis (Figure 1F). These results reveal that HHT may suppress HCC cell proliferation by arresting cells at the G2 phase.

HHT induces apoptosis of HCC cells. Cell death is deemed to be another key factor that leads to drug-induced mitigation of cancer cell growth [28]. After treating HCC cells with HHT, we used FITC-Annexin V/PI staining to study apoptosis and observed that the percentages of HCCLM3, HepG2, and Huh7 cells in the Q4 and Q2 quadrants, which represent early and late apoptotic cells, respectively, were elevated after HHT treatment in a dose-dependent manner (Figure 2A). When the HHT concentration was 40 nM, the total apoptosis rate of HCCLM3, HepG2, and Huh7 cells increased by 6-fold, 5-fold, and 2-fold compared with that of their corresponding control cells, respectively (Figure 2B). Western blot analysis also reported that the expression of Bax (a pro-apoptotic marker) increased in the HHT-treated HCC cells and that of Bcl-2 (an anti-apoptotic marker) decreased, indicating that the HHT-induced apoptosis is driven by an endogenous pathway (Figure 2C). Hence, the HHT-induced apoptosis may be a significant factor in the inhibition of HCC cell growth.

HHT inhibits the migration and invasion of HCC cells. Apart from inducing cancer cell apoptosis, many chemotherapies also have the ability to block tumor cell migration and invasion. Therefore, we used a wound-healing assay to elucidate the inhibitory effect of HHT on HCC cell migration. To avoid the influence of cell activity on cell migration, we used a lower concentration of HHT (0–10 nM) to discern the effect of HHT on migration, and mitomycin C to attenuate proliferation. Compared to the control group, the HHT-treated group had an effectively slower migration rate that was both, concentration- and time-dependent (Figures 3A, 3B). Consistently, the Transwell assays revealed a dose-dependent decline in the migration and invasion of HHT-treated HCC cells (Figures 3C, 3D). These results indicate that HHT treatment can inhibit the migration and invasion of HCC cells at non-cytotoxic concentrations.

HHT inhibits HCC progression *in vivo*. To evaluate the antitumor activity of HHT in HCC *in vivo*, we used BALB/c nude mice to establish an HCCLM3 xenograft tumor model. On day 14, the tumor weight and size in mice from the HHT-treated group were obviously smaller than those in mice from the control group, suggesting that HHT significantly inhibits tumor growth (Figures 4A and 4D–4F). USI and MRI technologies are non-invasive tools

that do not require radiation, do not increase mortality, and can provide detailed and accurate information for evaluating the effectiveness of tumor treatment. We used USI (B-mode, CDFI, CPA, and USE) and MRI (T1WI and T2WI) to monitor changes in the tumor. The ultrasound monitoring results showed that the tumor size, angiogenesis, and hardness index in the HHT treatment group were lower than those in the control group (Figure 4B). Furthermore, similar results were obtained by MRI with regard to tumor size (Figure 4C). H&E staining is a standard pathological method for assessing the efficacy of drugs. The results show that tumor growth and angiogenesis are ameliorated after HHT treatment. Furthermore, decreased immunohistochemical staining of the proliferation marker Ki67 (brown) and increased terminal deoxynucleotide transferase-mediated dUTP notch end labeling (TUNEL) staining (brown) revealed that proliferation was inhibited and apoptosis was increased in the HHT-treated HCCLM3 xenograft tumors (Figures 4G, 4H). To evaluate whether HHT had an adverse effect on mice, we collected heart, liver, spleen, lung, and kidney from both groups of mice. H&E staining demonstrated that compared with the control treatment, HHT treatment did not cause obvious necrosis in these organs (Figure 4I). To elucidate the role of HHT in metastasis *in vivo*, HCCLM3 cells were injected into nude mice via tail vein, and the mice were sacrificed 7 weeks later. The number of lung metastatic nodules was counted under a dissecting microscope. The results showed that compared with the control group, the HHT treatment group had fewer metastatic nodules (Figures 4J, 4K).

HHT suppresses EMT by repressing Slug expression in HCC cells. In addition to significant contribution to migration and invasion, EMT has also been reported to be a key mechanism for enhancing proliferation, memory, angiogenesis, and anti-apoptotic activity in cancer cells [8]. Consequently, we tried to evaluate the effect of HHT on EMT in HCC cells. The expression of key EMT biomarkers, including E-cadherin, N-cadherin, and Vimentin, was detected by western blot. The results showed that as the dose of HHT increased, the expression levels of the mesenchymal markers N-cadherin and Vimentin decreased while those of the epithelial marker E-cadherin increased (Figures 5A, 5B). These changes in N-cadherin, Vimentin, and E-cadherin expression indicated that interstitial to epithelial transformation, which is the reversal process of EMT, occurred after HHT treatment. At the same time, we investigated the expression of upstream EMT regulators, including Snail, Slug, and Twist, which have been reported to regulate EMT-related migration and invasion and play a role in promoting the proliferation and inhibiting apoptosis of tumor cells [11]. HHT treatment significantly suppressed the expression of Slug in a concentration-dependent manner in HCCLM3, HepG2, and Huh7 cells (Figures 5C, 5D), while there was no significant difference in the expression of Snail and Twist. Slug has been shown to be involved in

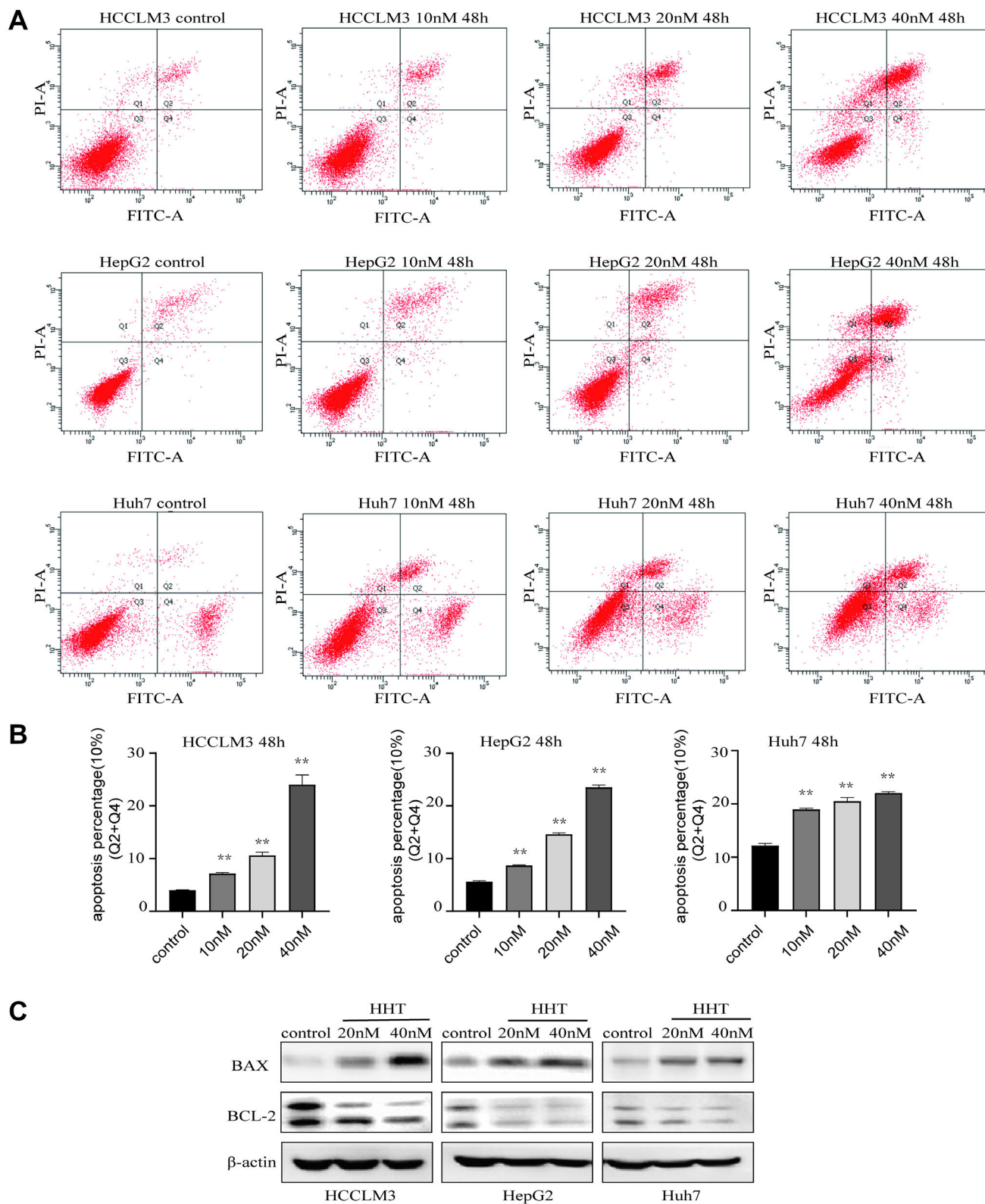
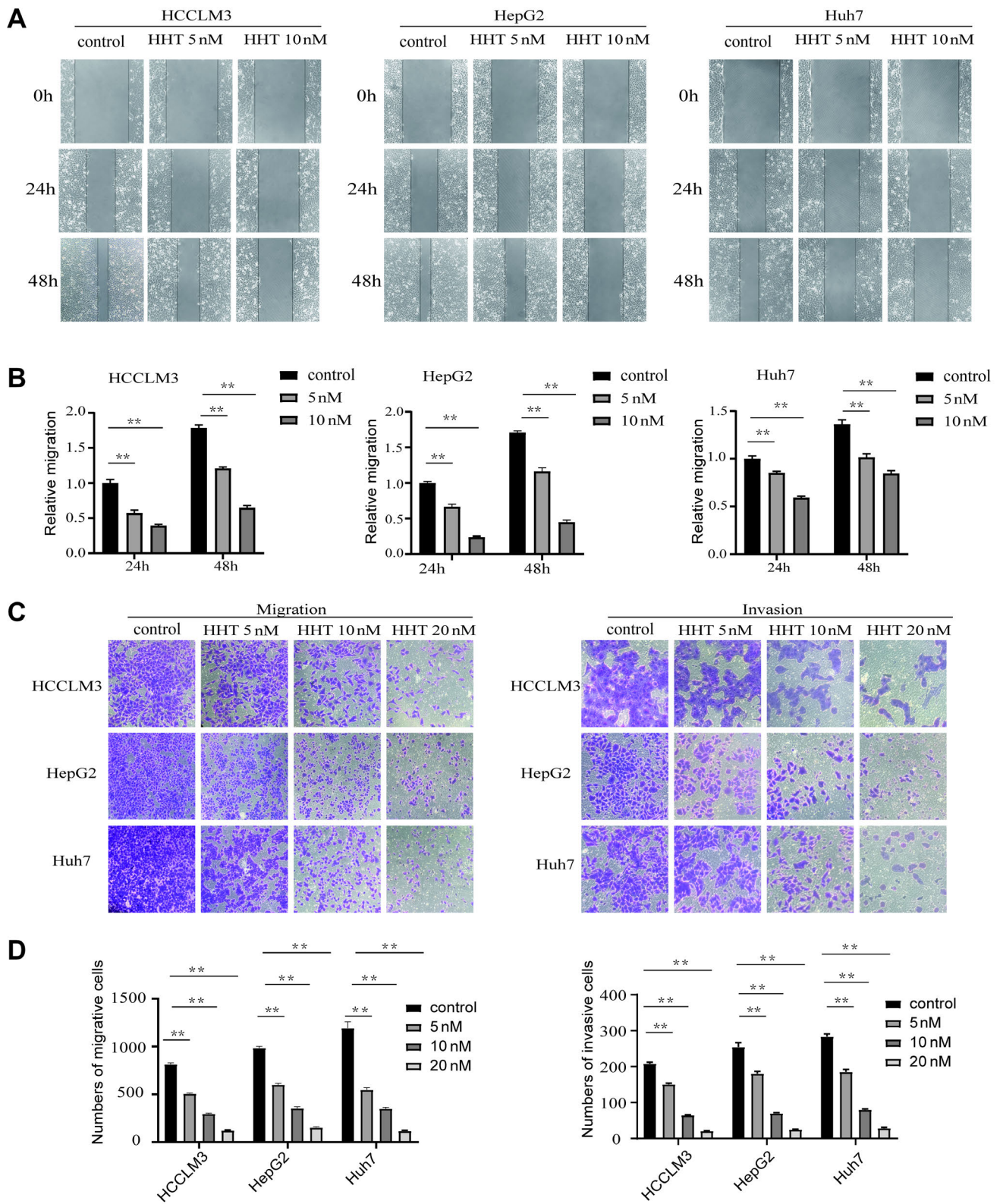
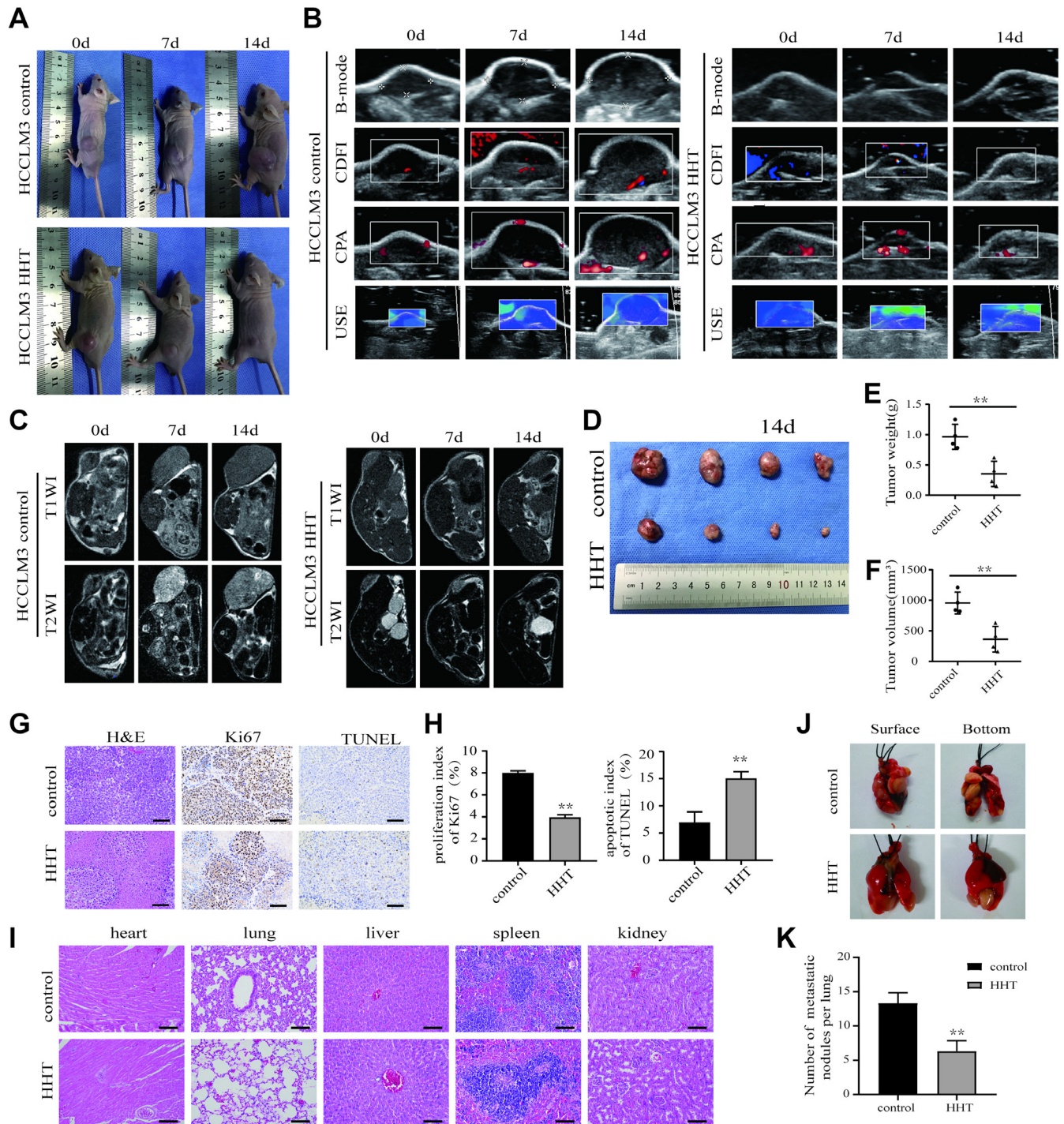
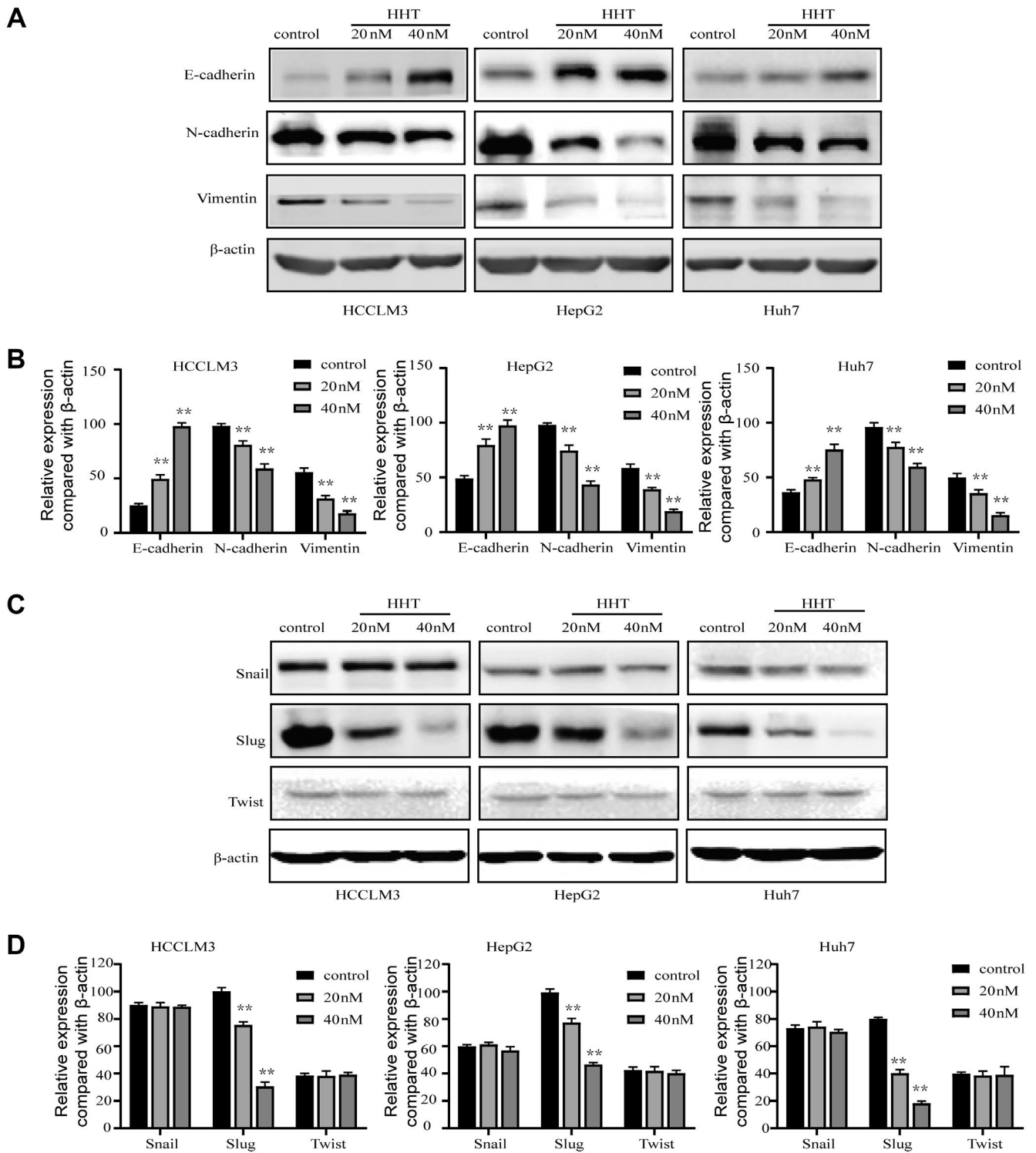


Figure 2. Apoptosis of HCC cells after treatment with HHT (0–40 nM, 48 h). A, B) Apoptosis assay of HCC cells treated with different concentrations of HHT (0–40 nM, 48 h). **p<0.01. C) Western blot assay indicated that Bcl-2 expression decreased and Bax expression increased in HCC cells treated with HHT (0–40 nM, 48 h). β-actin was used as the loading control.







EMT, proliferation, cell cycle progression, stem cell characteristics, angiogenesis, and anti-apoptotic activities [29]. These results show that HHT may exert the above-mentioned functions by inhibiting Slug-induced EMT.

HHT inhibits the PI3K/AKT signaling pathway in HCC cells. Accumulating evidence suggests that the PI3K/AKT pathway plays an important role in cell survival and metastasis [15, 30, 31]. Slug is a transcription factor that has been reported to be regulated by the PI3K/AKT signaling pathway in HCC cells in previous studies [32]. Therefore, we examined the expression and activation of key regulatory factors in this signaling pathway, including PI3K (p-PI3K) and AKT (p-AKT). The results showed that HHT significantly decreased the levels of phosphorylated PI3K and AKT in a dose-dependent manner, whereas the expression levels of total PI3K and AKT were not significantly different. GSK-3 β , as one of the downstream targets of AKT, mediates apoptosis [33]. Therefore, we examined GSK-3 β and its activated phosphorylated form (p-GSK-3 β) and discovered that HHT obviously reduced the levels of phosphorylated GSK-3 β in a dose-dependent manner (Figures 6A, 6B), but there was no significant difference in total GSK-3 β expression. Collectively, these data demonstrate that the inhibitory effect of HHT on the proliferation, migration, and invasion of HCC cells as well as the induction of apoptosis appears to act by inhibiting the PI3K/AKT/GSK-3 β /Slug signaling pathway.

AKT activator SC79 hindered the inhibitory effect of HHT on HCC. To further determine whether HHT suppresses the growth and metastasis of HCC via PI3K/AKT/GSK-3 β /Slug signaling, SC79, an activator of AKT, was used for rescue experiments. The results showed that compared with cells treated with HHT alone, cells treated with the combination of SC79 and HHT showed significant attenuation of the suppressive effect of HHT on cell proliferation (Figure 7A), migration, and invasion (Figures 7B–7D). We next investigated the effect of SC79 on the PI3K/AKT/GSK3 β /Slug signaling pathway and found that when SC79 was used in combination with HHT, the levels of p-AKT, p-GSK-3 β , and Slug were increased compared with those in response to HHT treatment alone (Figure 7E), indicating that the AKT activator SC79 can hinder the inhibitory effect of HHT on the levels of p-AKT, p-GSK-3 β , and Slug. This further proves that the inhibitory effect of HHT on the proliferation, migration, and invasion of HCC cells acts via suppression of the PI3K/AKT/GSK-3 β /Slug signaling pathway.

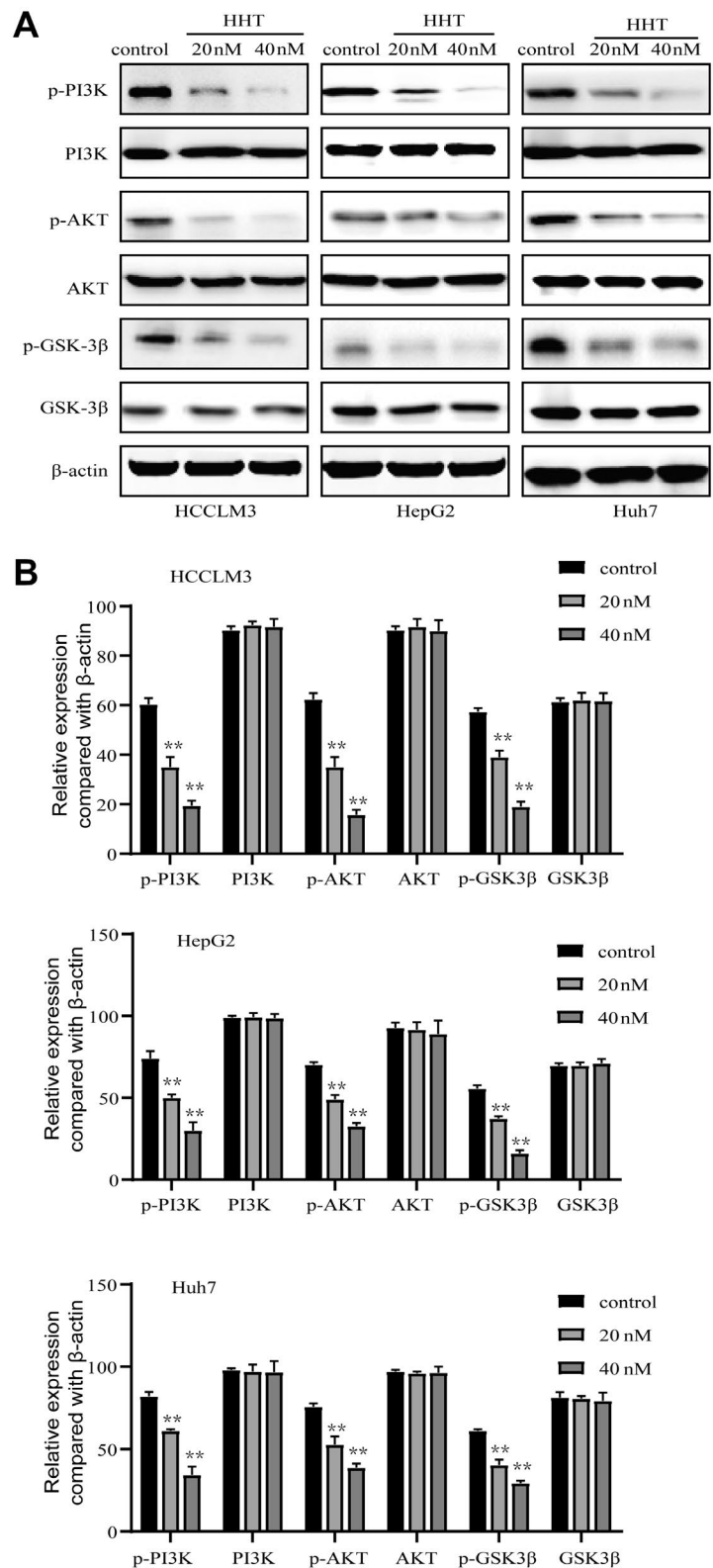


Figure 6. Expression of genes in the indicated signaling pathways in HCC cells after HHT treatment. A, B) Western blot of the expression of the primary proteins involved in key signaling pathways in cells treated with HHT (0–40 nM, 48 h). ** $p < 0.01$ vs. the control group (0 nM HHT).

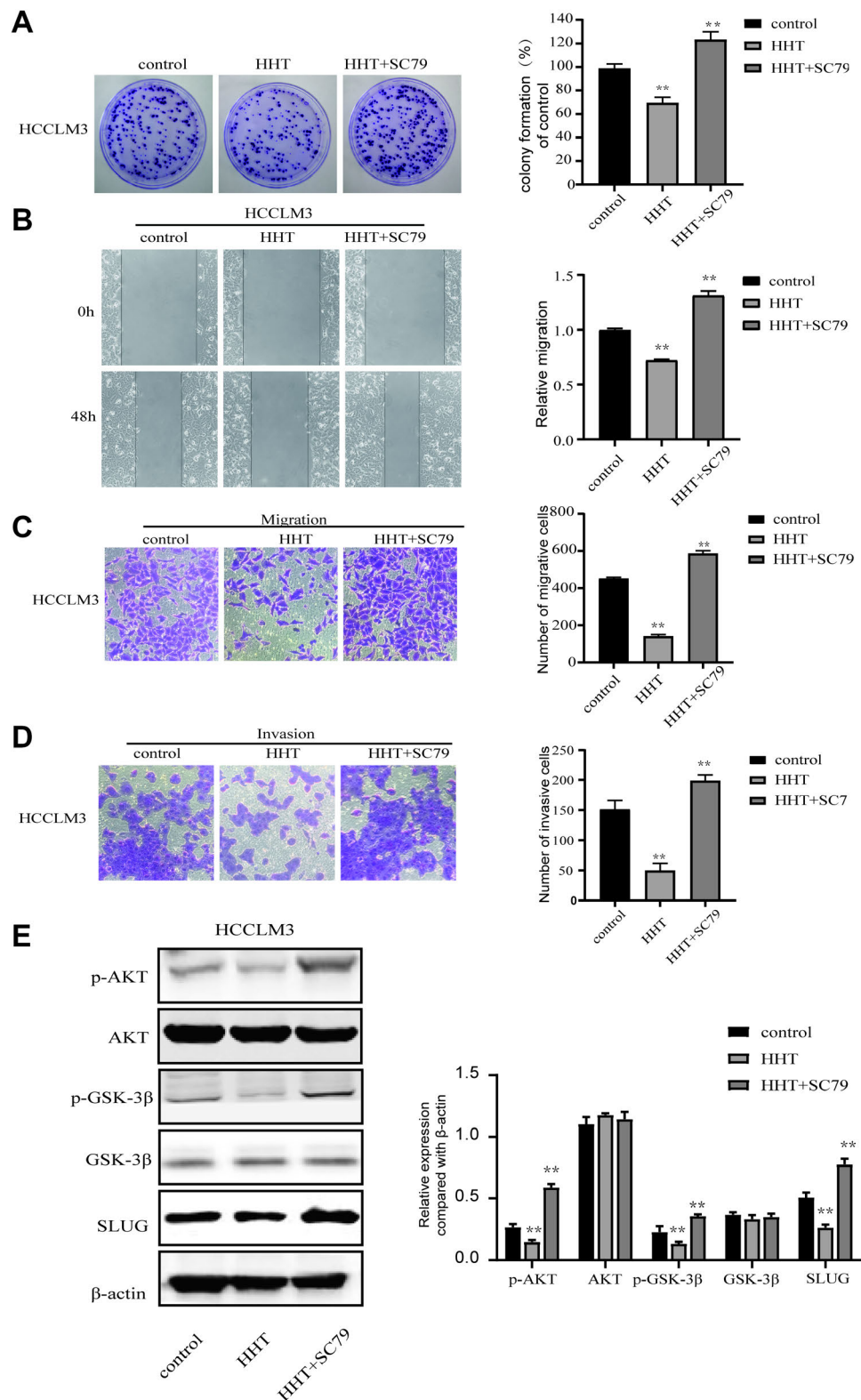


Figure 7. The AKT activator SC79 reversed the inhibitory effect of HHT on HCC cells. A) HCCLM3 cells were treated with HHT and/or SC79 and then analyzed by the colony formation assay. SC79 increased the viability of HHT-treated HCC cells. B–D) Wound-healing and Transwell assays indicated that, following the addition of SC79, the migration and invasion abilities of HCC cells were improved. E) After the addition of SC79, the levels of p-AKT, p-GSK-3 β , and Slug were elevated in HepG2 cells. ** $p < 0.01$ vs. the control group (0 nM HHT).

Discussion

The antitumor properties of natural metabolites and phytochemicals from plants have been receiving increasing attention [34]. HHT is a natural cephalotaxine alkaloid approved by the US Food and Drug Administration and has been used as an active antitumor agent in several kinds of cancers (Figure 8A). HHT can also be used to increase the sensitivity of drug-resistant cancer cells to apoptosis [35]. In this study, we determined that HHT could suppress the growth and metastasis of HCC both *in vitro* and *in vivo*, at least in part by inhibiting the PI3K/AKT/GSK-3 β /Slug signaling pathway.

In the present study, we found that HHT has potent anti-proliferative effects in three different HCC cell lines (HCCLM3, HepG2, and Huh7) in a dose-dependent manner. More importantly, our results showed that HHT could significantly inhibit the HCC activity at a low concentration, while the same inhibitory effect was obtained by sorafenib in the micromolar (μ M) range. In HCC cells, HHT inhibited colony formation, induced apoptosis, and arrested the cell cycle. The changes in the expression of the apoptosis-related proteins Bax and Bcl-2 and G2/M checkpoint protein Cyclin B1 further support these results. *In vivo*, xenograft tumor volume was monitored by USI and MRI, and reductions in

tumor size, angiogenesis, and stiffness index were observed in the HHT-treated group. Ki-67 expression and TUNEL staining also confirmed that HHT could inhibit the proliferation and induce apoptosis of HCCLM3 cells *in vivo*.

HCC migration and invasion are pivotal steps that lead to tumor metastasis and poor prognosis [36]. EMT has been shown to promote the metastatic ability, cell stemness, and metabolic alterations of HCC [37]. EMT is a complex and reversible biological process that shifts tumors from an epithelial-like phenotype to a mesenchymal-like phenotype, thereby increasing invasion and migration abilities [38, 39]. Functional assays confirmed that HHT suppresses the migration and invasion of HCC cells *in vitro*, and the number of lung metastases was lower in the HHT treatment group *in vivo*, indicating that HHT could reduce the metastatic ability of HCC cells. Downregulation of E-cadherin and upregulation of N-cadherin and Vimentin lead to an increase in cellular motility [40]. We further verified that HHT reversed EMT, which was illustrated by increases in E-cadherin expression and decreases in N-cadherin and Vimentin expression. In the next step, we sought to investigate how HHT affects the EMT phenotype. Because Snail, Slug, and Twist are pivotal EMT regulatory factors, we evaluated their expression patterns after HHT treatment. Slug was altered significantly in the HHT treatment group compared to the control group,

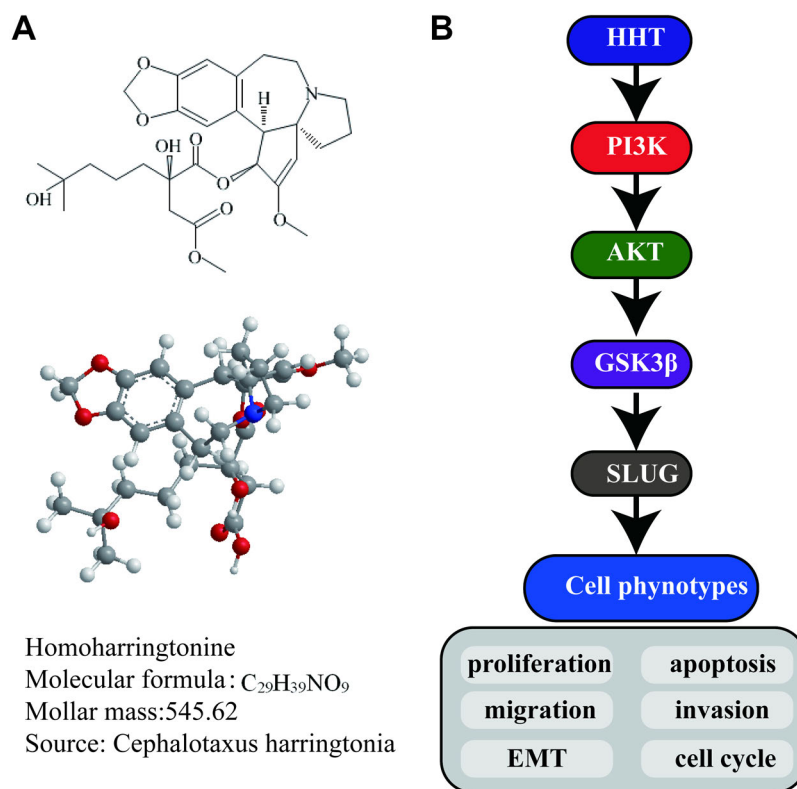


Figure 8. The chemical structure of HHT and its inhibitory mechanism of action in HCC. A) Chemical and 3D structure of HHT. B) Schematic diagram of the HHT-induced inhibitory activity in HCC and the relevant molecular mechanism referring to the PI3K/AKT/GSK-3 β /Slug signaling pathway.

indicating that HHT may inhibit migration and invasion at least in part by suppressing Slug-induced EMT.

To clarify the regulatory mechanisms by which HHT affects Slug, we examined the PI3K/AKT/GSK-3 β signaling pathway, which has been reported to regulate Slug [32]. Components of the PI3K/AKT/GSK-3 β signaling pathway are highly expressed in HCC cells and are related to clinicopathological characteristics, including differentiation, TNM stage, CLIP score, and lymphatic metastasis [41]. The PI3K/AKT/GSK-3 β axis participates in the proliferation, apoptosis, migration, invasion, and EMT of HCC cells [42–45]; hence, we assumed that HHT may inhibit Slug expression by acting on the PI3K/AKT/GSK-3 β signaling pathway. We observed that HHT decreased PI3K, AKT, and GSK-3 β activation, which indicated that the PI3K/AKT/GSK-3 β signaling pathway may mediate the effect of HHT on Slug. Moreover, the AKT activator SC79 partially rescued the proliferative, migratory, and invasive suppression of HHT in HCCLM3 cells. This evidence further supports the notion that HHT inhibits HCC proliferation and metastasis through the PI3K/AKT/GSK-3 β /Slug signaling pathway (Figure 8B).

In summary, this study indicates that HHT facilitates apoptosis and cell cycle arrest and inhibits cell invasion and metastasis of HCC by suppressing the PI3K/AKT/GSK-3 β /Slug signaling pathway. These findings suggest that HHT is a potential antitumor drug for HCC and that the PI3K/AKT/GSK-3 β /Slug signaling pathway plays an important role in the inhibitory effect of HHT on HCC. We will continue to explore whether there are other signaling pathways involved in this process.

Acknowledgments: This study was funded by the Natural Science Foundation of China (Grant No. 81871362).

References

- [1] KEW MC. Hepatocellular carcinoma: epidemiology and risk factors. *J Hepatocell Carcinoma* 2014; 1: 115–125. <https://doi.org/10.2147/JHC.S44381>
- [2] ZHANG J, CHEN Y, LIN J, JIA R, AN T et al. Cyclovirobuxine D Exerts Anticancer Effects by Suppressing the EGFR-FAK-AKT/ERK1/2-Slug Signaling Pathway in Human Hepatocellular Carcinoma. *DNA Cell Biol* 2020; 39: 355–367. <https://doi.org/10.1089/dna.2019.4990>
- [3] CHOI KJ, BAIK IH, YE SK, LEE YH. Molecular Targeted Therapy for Hepatocellular Carcinoma: Present Status and Future Directions. *Biol Pharm Bull* 2015; 38: 986–991. <https://doi.org/10.1248/bpb.b15-00231>
- [4] AVILA M, BERASAIN C. Making sorafenib irresistible: In vivo screening for mechanisms of therapy resistance in hepatocellular carcinoma hits on Mapk14. *Hepatology* 2015 May; 61: 1755–1757. <https://doi.org/10.1002/hep.27739>
- [5] HAN LL, YIN XR, ZHANG SQ. miR-103 promotes the metastasis and EMT of hepatocellular carcinoma by directly inhibiting LATS2. *Int J Oncol* 2018; 53: 2433–2444. <https://doi.org/10.3892/ijo.2018.4580>
- [6] LI Z, CHEN Y, AN T, LIU P, ZHU J et al. Nuciferine inhibits the progression of glioblastoma by suppressing the SOX2-AKT/STAT3-Slug signaling pathway. *J Exp Clin Cancer Res* 2019; 38: 139. <https://doi.org/10.1186/s13046-019-1134-y>
- [7] BRABLETZ T, KALLURI R, NIETO MA, WEINBERG RA. EMT in cancer. *Nat Rev Cancer* 2018; 18: 128–134. <https://doi.org/10.1038/nrc.2017.118>
- [8] NIETO MA, HUANG RY, JACKSON RA, THIERY JP. EMT: 2016. *Cell* 2016; 166: 21–45. <https://doi.org/10.1016/j.cell.2016.06.028>
- [9] SHIBUE T, WEINBERG RA. EMT, CSCs, and drug resistance: the mechanistic link and clinical implications. *Nat Rev Clin Oncol* 2017; 14: 611–629. <https://doi.org/10.1038/nrclinonc.2017.44>
- [10] PHILLIPS S, KUPERWASSER C. SLUG: critical regulator of epithelial cell identity in breast development and cancer. *Cell Adh Migr* 2014; 8: 578–587. <https://doi.org/10.4161/19336918.2014.972740>
- [11] VOUTSADAKIS IA. Epithelial-mesenchymal transition (EMT) and regulation of EMT factors by steroid nuclear receptors in breast cancer: a review and in silico investigation. *J Clin Med* 2016; 5: 11. <https://doi.org/10.3390/jcm5010011>
- [12] ALVES CC, CARNEIRO F, HOEFLER H, BECKER KF. Role of the epithelial mesenchymal transition regulator Slug in primary human cancers. *Front Biosci (Landmark Ed)* 2009; 14: 3035–3050. <https://doi.org/10.2741/3433>
- [13] HANAHAHAN D, WEINBERG RA. Hallmarks of cancer: the next generation. *Cell* 2011; 144: 646–674. <https://doi.org/10.1016/j.cell.2011.02.013>
- [14] FRESNO VARA JA, CASADO E, DE CASTRO J, CEJAS P, BELDA-INIESTA C et al. PI3K/Akt signalling pathway and cancer. *Cancer Treat Rev* 2004; 30: 193–204. <https://doi.org/10.1016/j.ctrv.2003.07.007>
- [15] CHAO X, ZAO J, XIAO-YI G, LI-JUN M, TAO S. Blocking of PI3K/AKT induces apoptosis by its effect on NF- κ B activity in gastric carcinoma cell line SGC7901. *Biomed Pharmacother* 2010; 64: 600–604. <https://doi.org/10.1016/j.biopha.2010.08.008>
- [16] MADDIKA S, ANDE SR, WIECHEC E, HANSEN LL, WESSELBORG S et al. Akt-mediated phosphorylation of CDK2 regulates its dual role in cell cycle progression and apoptosis. *J Cell Sci* 2008; 121: 979–988. <https://doi.org/10.1242/jcs.009530>
- [17] WOODGETT JR, OHASHI PS. GSK3: an in-Toll-erant protein kinase? *Nat Immunol* 2005; 6: 751–752. <https://doi.org/10.1038/ni0805-751>
- [18] SECA AML, PINTO DCGA. Plant Secondary Metabolites as Anticancer Agents: Successes in Clinical Trials and Therapeutic Application. *Int J Mol Sci* 2018; 19: 263. <https://doi.org/10.3390/ijms19010263>
- [19] KANTARJIAN HM, O'BRIEN S, CORTES J. Homoharringtonine/omacetaxine mepesuccinate: the long and winding road to food and drug administration approval. *Clin Lymphoma Myeloma Leuk* 2013; 13: 530–533. <https://doi.org/10.1016/j.clml.2013.03.017>
- [20] CHEN M, XIONG F, MA L, YAO H, WANG Q et al. Inhibitory effect of magnetic Fe3O4 nanoparticles coloaded with homoharringtonine on human leukemia cells in vivo and in vitro. *Int J Nanomedicine* 2016; 11: 4413–4422. <https://doi.org/10.2147/IJN.S105543>

- [21] WANG L, ZHAO L, WEI G, SAUR D, SEIDLER B et al. Homoharringtonine could induce quick protein synthesis of PSMD11 through activating MEK1/ERK1/2 signaling pathway in pancreatic cancer cells. *J Cell Biochem* 2018; 119: 6644–6656. <https://doi.org/10.1002/jcb.26847>
- [22] WOLFF NC, PAVÍA-JIMÉNEZ A, TCHEUYAP VT, ALEXANDER S, VISHWANATH M et al. High-throughput simultaneous screen and counterscreen identifies homoharringtonine as synthetic lethal with von Hippel-Lindau loss in renal cell carcinoma. *Oncotarget* 2015; 6: 16951–16962. <https://doi.org/10.18632/oncotarget.4773>
- [23] CAO W, LIU Y, ZHANG R, ZHANG B, WANG T et al. Homoharringtonine induces apoptosis and inhibits STAT3 via IL-6/JAK1/STAT3 signal pathway in Gefitinib-resistant lung cancer cells. *Sci Rep* 2015; 5: 8477. <https://doi.org/10.1038/srep08477>
- [24] BERANOVA L, POMBINHO AR, SPEGAROVA J, KOC M, KLANOVA M et al. The plant alkaloid and anti-leukemia drug homoharringtonine sensitizes resistant human colorectal carcinoma cells to TRAIL-induced apoptosis via multiple mechanisms. *Apoptosis* 2013; 18: 739–750. <https://doi.org/10.1007/s10495-013-0823-9>
- [25] ZHU M, GONG Z, WU Q, SU Q, YANG T et al. Homoharringtonine suppresses tumor proliferation and migration by regulating EphB4-mediated β -catenin loss in hepatocellular carcinoma. *Cell Death Dis* 2020; 11: 632. <https://doi.org/10.1038/s41419-020-02902-2>
- [26] LLOVET JM, RICCI S, MAZZAFERRO V, HILGARD P, GANE E et al. Sorafenib in advanced hepatocellular carcinoma. *N Engl J Med* 2008; 359: 378–390. <https://doi.org/10.1056/NEJMoa0708857>
- [27] GUZMÁN M. Effects on cell viability. *Handb Exp Pharmacol* 2005; 168: 627–642. https://doi.org/10.1007/3-540-26573-2_21
- [28] WANG J, CHEN S. RACK1 promotes miR-302b/c/d-3p expression and inhibits CCNO expression to induce cell apoptosis in cervical squamous cell carcinoma. *Cancer Cell Int* 2020; 20: 385. <https://doi.org/10.1186/s12935-020-01435-0>
- [29] ZHAO X, SUN B, SUN D, LIU T, CHE N et al. Slug promotes hepatocellular cancer cell progression by increasing sox2 and nanog expression. *Oncol Rep* 2015; 33: 149–156. <https://doi.org/10.3892/or.2014.3562>
- [30] FRESNO VARA JA, CASADO E, DE CASTRO J, CEJAS P, BELDA-INIESTA C et al. PI3K/Akt signalling pathway and cancer. *Cancer Treat Rev* 2004; 30: 193–204. <https://doi.org/10.1016/j.ctrv.2003.07.007>
- [31] YANG HY, HUANG CP, CAO MM, WANG YF, LIU Y. Long non-coding RNA CRNDE may be associated with poor prognosis by promoting proliferation and inhibiting apoptosis of cervical cancer cells through targeting PI3K/AKT. *Neoplasma* 2018; 65: 872–880. https://doi.org/10.4149/neo_2018_171225N841
- [32] LI Q, WANG C, WANG Y, SUN L, LIU Z et al. HSCs-derived COMP drives hepatocellular carcinoma progression by activating MEK/ERK and PI3K/AKT signaling pathways. *J Exp Clin Cancer Res* 2018; 37: 231. <https://doi.org/10.1186/s13046-018-0908-y>
- [33] SONG G, OUYANG G, BAO S. The activation of Akt/PKB signaling pathway and cell survival. *J Cell Mol Med* 2005; 9: 59–71. <https://doi.org/10.1111/j.1582-4934.2005.tb00337.x>
- [34] MISHRA BB, TIWARI VK. Natural products: an evolving role in future drug discovery. *Eur J Med Chem* 2011; 46: 4769–4807. <https://doi.org/10.1016/j.ejmech.2011.07.057>
- [35] PASIC I, LIPTON JH. Current approach to the treatment of chronic myeloid leukaemia. *Leuk Res* 2017; 55: 65–78. <https://doi.org/10.1016/j.leukres.2017.01.005>
- [36] ZHANG L, WANG Y, SUN J, MA H, GUO C. LINC00205 promotes proliferation, migration and invasion of HCC cells by targeting miR-122-5p. *Pathol Res Pract* 2019; 215: 152515. <https://doi.org/10.1016/j.prp.2019.152515>
- [37] LAMOUILLE S, CONNOLLY E, SMYTH JW, AKHURST RJ, DERYNCK R. TGF- β -induced activation of mTOR complex 2 drives epithelial-mesenchymal transition and cell invasion. *J Cell Sci* 2012; 125: 1259–1273. <https://doi.org/10.1242/jcs.095299>
- [38] ZHANG G, ZHANG G. Upregulation of FoxP4 in HCC promotes migration and invasion through regulation of EMT. *Oncol Lett* 2019; 17: 3944–3951. <https://doi.org/10.3892/ol.2019.10049>
- [39] WEI H, LIU Y, MIN J, ZHANG Y, WANG J et al. Protein arginine methyltransferase 1 promotes epithelial-mesenchymal transition via TGF- β 1/Smad pathway in hepatic carcinoma cells. *Neoplasma* 2019; 66: 918–929. https://doi.org/10.4149/neo_2018_181226N999
- [40] YANG Y, YAO JH, DU QY, ZHOU YC, YAO TJ et al. Connexin 32 downregulation is critical for chemoresistance in oxaliplatin-resistant HCC cells associated with EMT. *Cancer Manag Res* 2019; 11: 5133–5146. <https://doi.org/10.2147/CMAR.S203656>
- [41] ZHOU LJ, MO YB, BU X, WANG JJ, BAI J et al. Erinacine Facilitates the Opening of the Mitochondrial Permeability Transition Pore Through the Inhibition of the PI3K/ Akt/ GSK-3 β Signaling Pathway in Human Hepatocellular Carcinoma. *Cell Physiol Biochem* 2018; 50: 851–867. <https://doi.org/10.1159/000494472>
- [42] ZOU L, CHAI J, GAO Y, GUAN J, LIU Q et al. Down-regulated PLAC8 promotes hepatocellular carcinoma cell proliferation by enhancing PI3K/Akt/GSK3 β /Wnt/ β -catenin signaling. *Biomed Pharmacother* 2016; 84: 139–146. <https://doi.org/10.1016/j.biopha.2016.09.015>
- [43] SUN Y, GAO C, LUO M, WANG W, GU C et al. Aspidin PB, a phloroglucinol derivative, induces apoptosis in human hepatocarcinoma HepG2 cells by modulating PI3K/Akt/GSK3 β pathway. *Chem Biol Interact* 2013; 201: 1–8. <https://doi.org/10.1016/j.cbi.2012.11.005>
- [44] ZHOU SL, ZHOU ZJ, HU ZQ, LI X, HUANG XW et al. CXCR2/CXCL5 axis contributes to epithelial-mesenchymal transition of HCC cells through activating PI3K/Akt/GSK-3 β /Snail signaling. *Cancer Lett* 2015; 358: 124–135. <https://doi.org/10.1016/j.canlet.2014.11.044>
- [45] JIANG H, ZHOU Z, JIN S, XU K, ZHANG H et al. PRMT9 promotes hepatocellular carcinoma invasion and metastasis via activating PI3K/Akt/GSK-3 β /Snail signaling. *Cancer Sci* 2018; 109: 1414–1427. <https://doi.org/10.1111/cas.13598>